doi:10.1111/evo.14308

Ecdysis-related neuropeptide expression and metamorphosis in a non-ecdysozoan bilaterian

Elisabeth Zieger,[1,2] Andrew D. Calcino,[1] Nicolas S.M. Robert,[3] Christian Baranyi,[1] and Andreas Wanninger[1,4]

[1]*Department of Evolutionary Biology, Unit for Integrative Zoology, University of Vienna, Vienna, Austria*

[2]*E-mail: elisabeth.zieger@univie.ac.at*

[3]*Department of Neuroscience and Developmental Biology, University of Vienna, Vienna, Austria*

[4]*E-mail: andreas.wanninger@univie.ac.at*

Received April 28, 2021
Accepted June 29, 2021

Ecdysis-related neuropeptides (ERNs), including eclosion hormone, crustacean cardioactive peptide, myoinhibitory peptide, bursicon alpha, and bursicon beta regulate molting in insects and crustaceans. Recent evidence further revealed that ERNs likely play an ancestral role in invertebrate life cycle transitions, but their tempo-spatial expression patterns have not been investigated outside Arthropoda. Using RNA-seq and *in situ* hybridization, we show that ERNs are broadly expressed in the developing nervous system of a mollusk, the polyplacophoran *Acanthochitona fascicularis*. While some ERN-expressing neurons persist from larval to juvenile stages, others are only present during settlement and metamorphosis. These transient neurons belong to the "ampullary system," a polyplacophoran-specific larval sensory structure. Surprisingly, however, ERN expression is absent from the apical organ, another larval sensory structure that degenerates before settlement is completed in *A. fascicularis*. Our findings thus support a role of ERNs in *A. fascicularis* metamorphosis but contradict the common notion that the apical organ-like structures shared by various aquatic invertebrates (i.e., cnidarians, annelids, mollusks, echinoderms) are of general importance for this process.

KEY WORDS: Apical organ, invertebrate development and evolution, life cycle, sensory neurons, settlement and metamorphosis.

In order to grow, some animals need to shed their exoskeleton. This process is commonly termed "ecdysis" and probably originated in the last common ancestor of Ecdysozoa, an invertebrate superphylum including Scalidophora, Nematoda, and Panarthropoda (Wang et al. 2019). In the fruit fly *Drosophila melanogaster* and the moth *Manduca sexta*, molting involves innate pre-ecdysis, ecdysis, and post-ecdysis motor behaviors that are controlled by a cascade of ecdysis-regulating neuropeptides (ERNs) (Ewer 2005; Zitnan and Adams 2012; White and Ewer 2014; Kim et al. 2015; Nässel and Zandawala 2019). Key ERNs include eclosion hormone (EH), crustacean cardioactive peptide (CCAP), myoinhibitory peptide (MIP), bursicon alpha (Bursα), and bursicon beta (Bursβ). Several studies indicate that these neuropeptides also contribute to molting in hemimetabolous insects and crustaceans (Lee et al. 2013; Webster et al. 2013; Lenaerts et al. 2017; Zhou et al. 2017; Oliphant et al. 2018; Wulff et al. 2018). Interestingly, however, most of them have been lost in nematodes (de Oliveira et al. 2019).

Notably, ERNs are not limited to coordinating ecdysis-related processes. CCAP exerts excitatory effects on heartbeat frequency, oviduct contractions, and the secretion of digestive enzymes in arthropods (Žitňan and Daubnerová 2016), while MIP inhibits muscular contractions, regulates feeding and reproductive behavior, and integrates developmental timing with environmental cues in numerous bilaterians (Shao et al. 2019; Williams 2020). Bursα homodimers contribute to stem cell quiescence in *Drosophila* (Scopelliti et al. 2016), while Bursα and Bursβ homodimers contribute to neuroendocrine-immune responses of both insects and crustaceans (An et al. 2012; Zhang et al. 2017, 2020; Li et al. 2019). Although EH involvement in processes

other than ecdysis has not yet been described, these findings illustrate that ERNs generally serve multiple functions. Given that they are not only present in ecdysozoans, but also in the two remaining, non-molting bilaterian superphyla, Lophotrochozoa and Deuterostomia, it is likely that ecdysis regulation is a derived function of ERNs that emerged during early ecdysozoan evolution (de Oliveira et al. 2019; Zieger et al. 2020).

Based on their temporal expression profiles, it has been suggested that ERNs play a conserved role in nephrozoan (Protostomia + Deuterostomia) life cycle transitions such as hatching in direct-developing species or metamorphosis in indirect developers (Zieger et al. 2020). However, *in situ* evidence for ERN expression in a non-ecdysozoan is currently lacking. This study provides the first documentation, to our knowledge, of ERN-expressing cells in key developmental stages of the polyplacophoran mollusk *Acanthochitona fascicularis*. Polyplacophorans have a fossil record that dates back ~ 500 mya and exhibit a number of mollusk-specific and putatively ancestral features (Vinther et al. 2012; Scherholz et al. 2013; Vinther 2015; Wanninger and Wollesen 2019), including a non-ganglionated tetraneurous nervous system composed of an anterior circumoesophageal nerve ring and four main longitudinal nerve cords that are interconnected via commissures (Wanninger 2009; Richter et al. 2010; Sigwart et al. 2014; Fritsch et al. 2016).

During polyplacophoran larval development, the scaffold of the adult nervous system is established through successive formation of cerebral, pedal, and lateral neurons (Friedrich et al. 2002; Voronezhskaya et al. 2002). Interestingly, this does not occur in an anterior-to-posterior progression, in contrast to segmented lophotrochozoans such as Annelida (Friedrich et al. 2002). The non-feeding polyplacophoran trochophore further possesses sensory structures that are restricted to the larval stage, including an apical organ and a so-called anterolateral "ampullary system" (Friedrich et al. 2002; Haszprunar et al. 2002; Voronezhskaya et al. 2002). Apical organ-like structures are found in many aquatic invertebrate larvae, including those of cnidarians, lophotrochozoans, and deuterostomes, where they are thought to regulate locomotion, settlement, and metamorphosis (Kempf et al. 1997; Hadfield et al. 2000; Voronezhskaya and Khabarova 2003; Voronezhskaya et al. 2004; Rentzsch et al. 2008; Conzelmann et al. 2013; Hou et al. 2020). The ampullary system, on the other hand, is probably a polyplacophoran-specific feature of yet unknown function (Friedrich et al. 2002; Haszprunar et al. 2002; Voronezhskaya et al. 2002).

Here, we used immunofluorescence, RNA-seq differential expression analysis, and *in situ* hybridization to assess ERN expression in the developing nervous system of a non-ecdysozoan animal, the polyplacophoran mollusk *Acanthochitona fascicularis*. Our data shed new light on the dynamic roles of neuropeptides and larval sensory systems in animal life cycle transitions and contradict common assumptions concerning the involvement of the apical organ in settlement and metamorphosis.

Material and Methods

ANIMAL COLLECTION, CULTURE, AND FIXATION

Adult specimens of *Acanthochitona fascicularis* were collected in the intertidal zone near the Station Biologique de Roscoff in France (48°43´44.70"N 3°59´13.53"W). The animals spawned spontaneously at room temperature (20-22°C) 2 to 4 days after collection. After adding several drops of concentrated sperm solution and incubation for 40 min, eggs were washed and reared in filtered seawater at room temperature. Late trochophore larvae (48-60 h) were provided with empty gastropod shells from the collection site to induce settlement and metamorphosis (Wanninger and Haszprunar 2002). For immunofluorescence, specimens were fixed in 4% PFA in PBS (0.01 M phosphate buffered saline, pH 7), washed three times in PBS, and stored at 4°C in PBS containing 0.1% sodium azide. For RNA extraction, water was removed by centrifugation and developmental stages were flash-frozen in liquid nitrogen and stored at -80°C. For *in situ* hybridization, larvae and juveniles were fixed in 4% PFA in MOPS-EGTA (0.1 M MOPS, 2 mM MgSO4, 1 mM EGTA, 0.5 M NaCl) for 1–2 h, washed three times in 100% methanol, and stored in methanol containing 50 mM EGTA at -20°C.

IMMUNOFLUORESCENCE AND IMAGING

Developmental stages of *Acanthochitona fascicularis* were labeled according to established protocols (Pavlicek et al. 2018) using mouse anti-acetylated α-tubulin diluted 1:800 (Sigma; St. Louis; MO, USA), rabbit anti-5-HT diluted 1:1000 (Immunostar; Hudson, WI, USA) and HOECHST diluted 1:5000 (Sigma-Aldrich; St. Louis; MO, USA) in blocking buffer (PBS containing 0.1 % Tween 20 (#9127.1, Carl Roth) and 3% normal goat serum (Invitrogen; Molecular Probes, Eugene, OR, USA)). Specimens were mounted on glass slides in Fluoromount-G (Southern Biotech, Birmingham, AL, USA), stored at 4°C, and imaged using a confocal laser scanning microscope (DMI6000 CFS, TCS SP5 II, Leica Microsystems, Wetzlar, Germany). Maximum projections of image stacks were generated and global brightness and contrast were adjusted in ImageJ (Schneider et al. 2012).

SEQUENCING AND TRANSCRIPTOME ASSEMBLY

RNA was extracted from samples stored at -80°C in RNAlater (AMBION, Inc., Austin, Texas) using the RNeasy® Plus Mini kit (74134, QIAGEN, Hilden, Germany). RNA-seq libraries were constructed for each sample using the NEBNext® Ultra™ II Directional RNA Library Prep Kit (#E7760, New England Biolabs, Frankfurt am Main, Germany) and the samples were multiplexed and sequenced on an Illumina NovaSeq 6000 using the

SP protocol. Both library prep and sequencing were performed by the Next Generation Sequencing Facility at Vienna BioCenter Core Facilities (VBCF), member of the Vienna BioCenter (VBC), Austria.

For command line details of all bioinformatic steps, see Data S1, Supplementary Information). Libraries were preprocessed with bbduk (version 37.61, BBMap. http://www.sourceforge.net/projects/bbmap/) to remove low-quality bases and adapter sequences (Bushnell et al. 2017). Library quality was assessed with fastqc (version 0.11.8, www.bioinformatics.babraham.ac.uk/projects/fastqc/). De novo transcriptomes were built for each developmental stage with transabyss (version 2.0.1) (Robertson et al. 2010) and these were then merged with transabyss-merge. Open reading frames were annotated with TransDecoder (version 5.02) (Haas et al. 2013) and redundancy of the output was reduced by using cd-hit (version 4.8.1) (Li and Godzik 2006) . Only those transcripts that encoded a peptide with a complete start and stop codon were retained for further analysis. It was noticed that no orthologue of eclosion hormone passed the stringent filtering performed during transcriptome construction, however a complete EH was found in the concatenated transcriptome file prior to ORF annotation. As such, EH was manually annotated and added to the reference transcriptome, bringing it to a total of 27,263 genes.

NEUROPEPTIDE ANNOTATION AND QUANTIFICATION OF TRANSCRIPT ABUNDANCE

Using previously annotated neuropeptide sequences as queries (De Oliveira et al. 2019; de Oliveira et al. 2019; Zieger et al. 2020), *Acanthochitona fascicularis* orthologues of eclosion hormone (EH), crustacean cardioactive peptide (CCAP), myoinhibitory peptide (MIP), bursicon alpha (Bursα) and bursicon beta (Bursβ) were retrieved through BLAST searches with default tBLASTn parameters and an e-value threshold of 1. Candidate sequences were checked by reciprocal BLASTs and aligned with their respective bilaterian orthologues using the EINSI algorithm of MAFFT (Katoh and Standley 2013). Sequence orthology was initially determined based on the presence of shared conserved amino acid regions and residues (Figure S1, Supplementary Information). EH and Burs pro-neuropeptide sequences are characterized by a pattern of six and eleven conserved cysteine residues, respectively (except polychaete, scaphopod and cnidarian EH with only five cysteine residues), CCAP by a K-R-x-F-C-N-x(3)-F-T-G-C motif and MIP by a repeated W-x(5,6,7)-WGKR motif (Žitňan et al. 2007; Conzelmann et al. 2013; de Oliveira et al. 2019; De Oliveira et al. 2019; Zieger et al. 2020). Alignments and histograms were produced in Jalview (Waterhouse et al. 2009). Sequence annotation was confirmed through phylogenetic analyses (Figure S1, Supplementary Information). For each alignment, best fitting models were determined using ModelFinder (Kalyaanamoorthy et al. 2017). Accordingly, Maximum Likelihood (ML) trees were inferred using IQTREE v1.6.2 (Nguyen et al. 2015) with the VT+R3, VT+I+G4, PMB+G4, and rtREV+F+R3 models for the Bursα/β, CCAP, EH, and MIP trees, respectively. Node support of the ML trees was estimated by 200 bootstrap pseudoreplicates and by Shimodaira-Hasegawa approximate Likelihood Ratio Test. Bayesian Inference trees were inferred using the LG+G4, WAG+G4, WAG +G4, and mtREV+G4 models in PhyloBayes 4.1c (Lartillot et al. 2009) for the Bursα/β, CCAP, EH, and MIP trees, respectively. Two independent chains were run simultaneously for 10000 cycles and convergence was checked using the maxdiff parameter (< 0.1). A majority-rule consensus tree was then built using a sample of 900 trees per chain, discarding the first 10% of the trees as burn-in. ML and BI phylograms were edited in FigTree (http://tree.bio.ed.ac.uk/software/figtree/).

Transcript abundances were quantified as TPMs (Transcripts Per Kilobase Million) using Kallisto (Bray et al. 2016).

IN SITU HYBRIDIZATION AND IMAGING

Gene-specific primers (Data S2, Supplementary Information) were designed using OligoCalc (Kibbe 2007). PCR amplification, cloning, and ligation were performed as previously described (Fritsch et al. 2015). Probes were generated using digoxigenin and fluorescein RNA Labelling kits (#11277073910 and #11685619910, Roche Diagnostics GmbH, Mannheim, Germany). Probe sequences are provided in (Data S2, Supplementary Information). Whole-mount *in situ* hybridization was performed as previously described (Fritsch et al. 2015, 2016), but with a probe concentration of 1 ng/μL and a hybridization temperature of 58°C. Larvae were incubated in digoxigenin or fluorescein antibodies conjugated to alkaline phosphatase (#11093274910 and # 11426338910 Roche, 1:3000 dilution) for 24 h at 4°C.

For single *in situ* hybridization, the color reaction was carried out in alkaline phosphatase buffer (APB, Tris-HCl, 100 mM, pH 9.5) containing 7.5% polyvinyl alcohol and 2% NBT/BCIP (#11681451001, Roche) for 1–6 h. After successful staining, larvae were washed in PBT (0.1 M phosphate buffered saline, 0.1% Tween-20, pH 7), cleared in a 1:1 benzylalcohol:benzylbenzoate solution (Fritsch et al. 2015) and imaged with a Nikon Eclipse E800 microscope and a Nikon Fi2-U3 camera.

For double *in situ* hybridization, the fluorescein-labeled probe was visualized first, using 250 μg/ml Fast Blue BB Salt (F3378, Sigma, Darmstadt, Germany) and 250 μg/ml 3-hydroxy-2-naphtoic acid (N5000, Sigma) in APB-containing 50 mM $MgCl_2$ (pH 8.5). Prior to the second detection round, larvae were washed in PBT and the fluorescein antibody conjugate was inactivated by 0.1 M glycine-HCl (pH 2.2) treatment at 60°C for 15 min. The second digoxigenin-labeled probe was visualized

using a SIGMAFAST™ Fast Red/Naphthol tablet (F4648, Sigma) in 1 ml APB containing 50 mM $MgCl_2$ (pH 8.5). For co-detection of ERN gene expression, larvae were mounted in glycerol containing 0.1 M phosphate-buffered saline and 0.25 % DABCO (D27802, Sigma, Darmstadt, Germany). Fast Blue and Fast Red fluorescence were detected using a confocal laser scanning microscope (DMI6000 CFS, TCS SP5 II, Leica Microsystems, Wetzlar, Germany).

RESULTS

ERN EXPRESSION IS STRONGLY UPREGULATED AT SETTLEMENT AND METAMORPHOSIS

RNA-seq data from six embryonic, six larval, and two juvenile stages of the polyplacophoran mollusk *Acanthochitona fascicularis* was pseudo-aligned and quantified as TPM (transcripts per million) values in order to compare ERN transcript levels throughout development (Fig. 1a). ERN expression is first upregulated in late trochophore stages and strongly increases during settlement and metamorphosis. In juveniles, ERN transcript levels decrease only slightly. These results correspond well to our *in situ* hybridization data (Figs. 2–7). ERNs with high TPM values are expressed by more neurons than ERNs with lower TPM values (e.g., *MIP* by 24 neurons and *Burs*β by only two neurons).

ONTOGENY AND METAMORPHOSIS OF THE *ACANTHOCHITONA FASCICULARIS* NERVOUS SYSTEM

Key steps of *A. fascicularis* development were documented with special focus on larval settlement, using serotonin (5-HT) and acetylated alpha-tubulin as markers for neurogenesis and for stage-dependent changes in ciliation.

Within 24 h after fertilization, *A. fascicularis* embryos reach the early trochophore stage (Fig. 1c). The trochophores possess a well-developed apical tuft and a ciliated prototroch, which persist throughout the free-swimming larval phase. Several 5-HT-like immunoreactive (5-HT-lir) cells are present, including four flask-shaped sensory neurons that belong to the apical organ (AO, Fig. 1c) and four ventral sensory neurons (VS, Fig. 1c). All of these neurons project to the cerebral commissure. During later trochophore stages (Fig. 1d,e,h), the number of flask-shaped sensory neurons in the apical organ increases to six and numerous 5-HT-lir somata are detected along the ventral nerve cords. In addition, a pair of dorsolateral 5-HT-lir sensory neurons (DLS, Fig. 1e) is present near the approximate location of the ampullary system, a polyplacophoran-specific larval sensory complex (Friedrich et al. 2002; Haszprunar et al. 2002). 5-HT-lir neurites can further be observed in the cerebral commissure, the circumesophageal nerve ring, the prototrochal nerve grid, the ventral and lateral nerve cords, and in the commissures that interconnect the main nerve cords.

The onset of settlement (Fig. 1h-l) is characterized by the almost instantaneous loss of the apical tuft, the prototroch, the apical organ, the prototrochal nerve grid, as well as the dorsolateral and the ventral sensory neurons (Fig. 1h-l). Presence of these structures thus overlaps precisely with the duration of larval swimming in *A. fascicularis*. Formation of the ciliated foot sole also progresses quickly during early settlement stages (Fig. 1k). Newly settled juveniles (Fig. 1g) lack 5-HT-lir epidermal sensory neurons, but do possess additional somata that exhibit weak 5-HT-lir around the cerebral commissure and a denser network of 5-HT-lir neurites that innervates the foot.

ERNS ARE DYNAMICALLY EXPRESSED IN INDIVIDUALLY IDENTIFIABLE NEURONS

In *A. fascicularis*, ERN expression starts around the mid-trochophore stage and is particularly prominent in metamorphic competent trochophores (Figs. 2–3) and settlement stages (Figs. 4–6). All ERNs are expressed in individually identifiable cells that can be traced throughout development. These cells are most likely neurons, since they are arranged in bilaterally symmetrical pairs that localize to major nervous system structures, such as the cerebral commissure, the ampullary system, and the ventral and lateral nerve cords. However, since *in situ* hybridization rarely labels neurites, it is possible that some cells correspond to endocrine cells instead. Most ERN-expressing neurons occupy basi-epidermal positions and their distribution patterns are highly consistent between specimens (Fig. 2–7). ERN-expressing neurons in the episphere (larval region anterior to the prototroch) are mostly flask-shaped, suggesting sensory roles. Notably, however, no ERN expression could be detected in the apical organ. After settlement and metamorphosis, several ERN neurons are lost together with parts of the episphere, whereas others are retained in early juveniles (Figs. 2–3).

Eclosion hormone

Eclosion hormone (*EH*) expression begins in the mid-trochophore stage in two pairs of bilaterally symmetrical neurons (e4/5) that are situated in the lateral epidermis of the episphere (Fig. 2a). In late trochophores, three more pairs of *EH* neurons are present in the vicinity of e4/5 (Fig. 2b-c,e), one in a basi-epidermal position (e1) and two in proximity to the brain (e2/3). The basi-epidermal neurons are flask-shaped and belong to the so-called ampullary system (Fig. 2), a larval sensory complex that is autapomorphic for Polyplacophora (Friedrich et al. 2002; Haszprunar et al. 2002). Another three to four pairs of *EH*-expressing neurons are distributed in the hyposphere along the ventral nerve cords, with the anterior-most pair being located just posterior to the prototroch (e6-9, Fig. 2b-c,e). In early

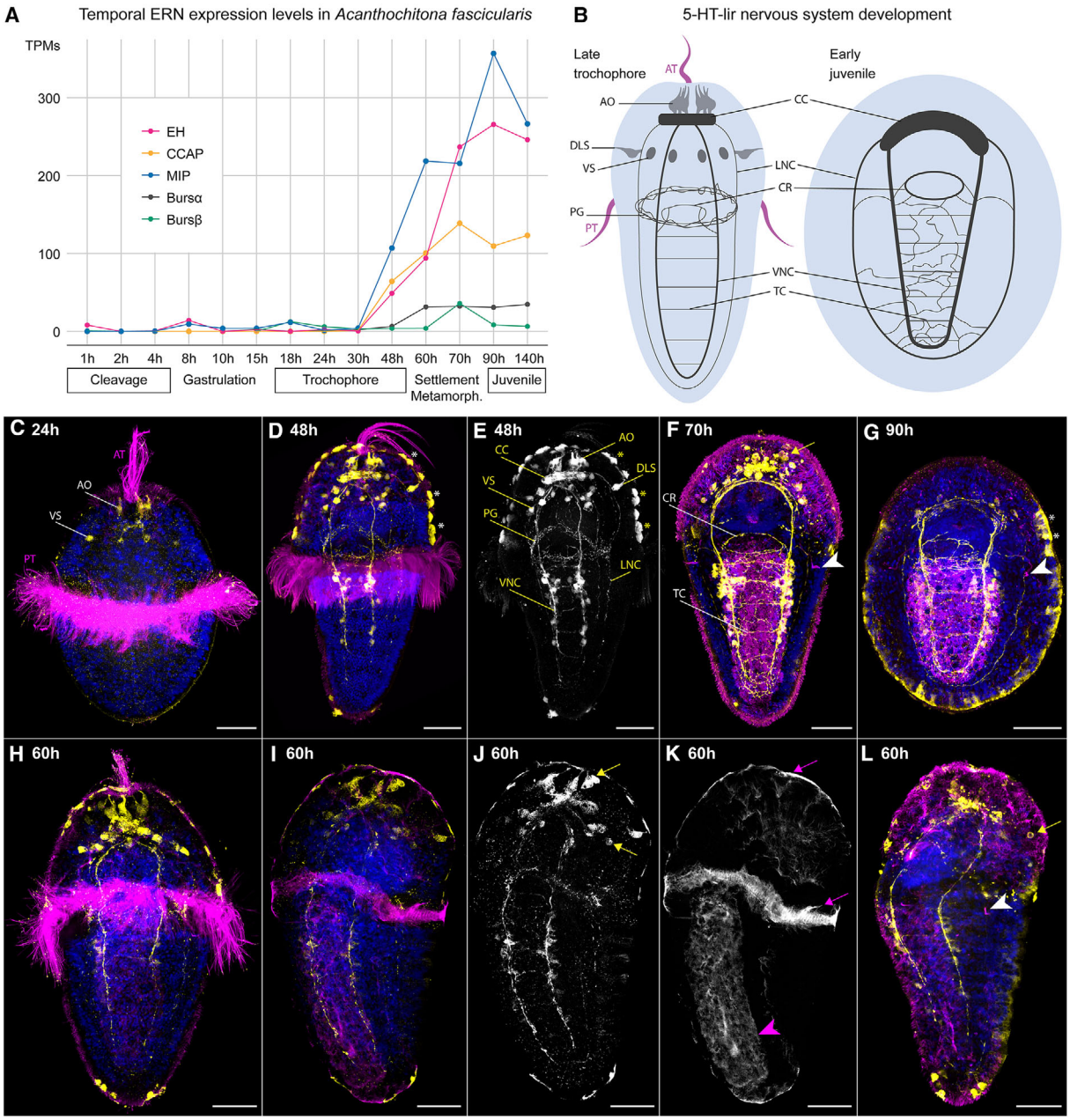

Figure 1. Ecdysis-related neuropeptide (ERN) expression profiles and serotonin-like immunoreactivity during ontogeny of *Acanthochitona fascicularis*. (A) Line graph shows the TPM values (transcripts per million) of each ERN in 14 developmental stages from early cleavage to late juvenile. (B) Schematic ventral view of major serotonin-like immunoreactive (5-HT-lir) cells and neurites (dark grey) in a late trochophore and in an early juvenile. Epidermal sensory neurons are mostly flask-shaped and transient neurons are semi-transparent. (C-L) 5-HT-lir (yellow) and acetylated alpha-tubulin-lir (magenta) in key stages of neurogenesis, including early trochophore (C), late trochophore (D-E), recently settled larva (F), and early juvenile (H, G). All specimens are shown in ventral view with their apical side oriented upwards. Hoechst-labeled nuclei are shown in blue and asterisks (*) mark unspecific fluorescence of epidermal secretory cells. Grey scale images display only a single immunofluorescent channel, either for 5-HT-lir (E,J) or for acetylated alpha-tubulin-lir (K). (H-L) The onset of settlement at 60 h is characterized by rapid changes. Many epidermal neurons lose their flask-like shape, become round and disintegrate (J,L, yellow arrows), resulting in the loss of the apical organ, the prototrochal nerve grid and of several dorsolateral and ventral sensory neurons (F,G,L). The apical tuft and prototroch cilia are also lost (K, magenta arrows), whereas new cilia are formed in the developing nephridia (F,G,L, white arrowheads) and on the foot (K, magenta arrowhead). Scale bars: 50 μm. Abbreviations: AO, apical organ, AT, apical tuft, CC, cerebral commissure, CR, circumesophageal nerve ring, DLS, dorsolateral sensory neuron, LNC, lateral nerve chord, PG, prototrochal grid, PT, prototroch, TC, transverse commissure, VNC, ventral nerve cord, VS, ventral sensory neurons.

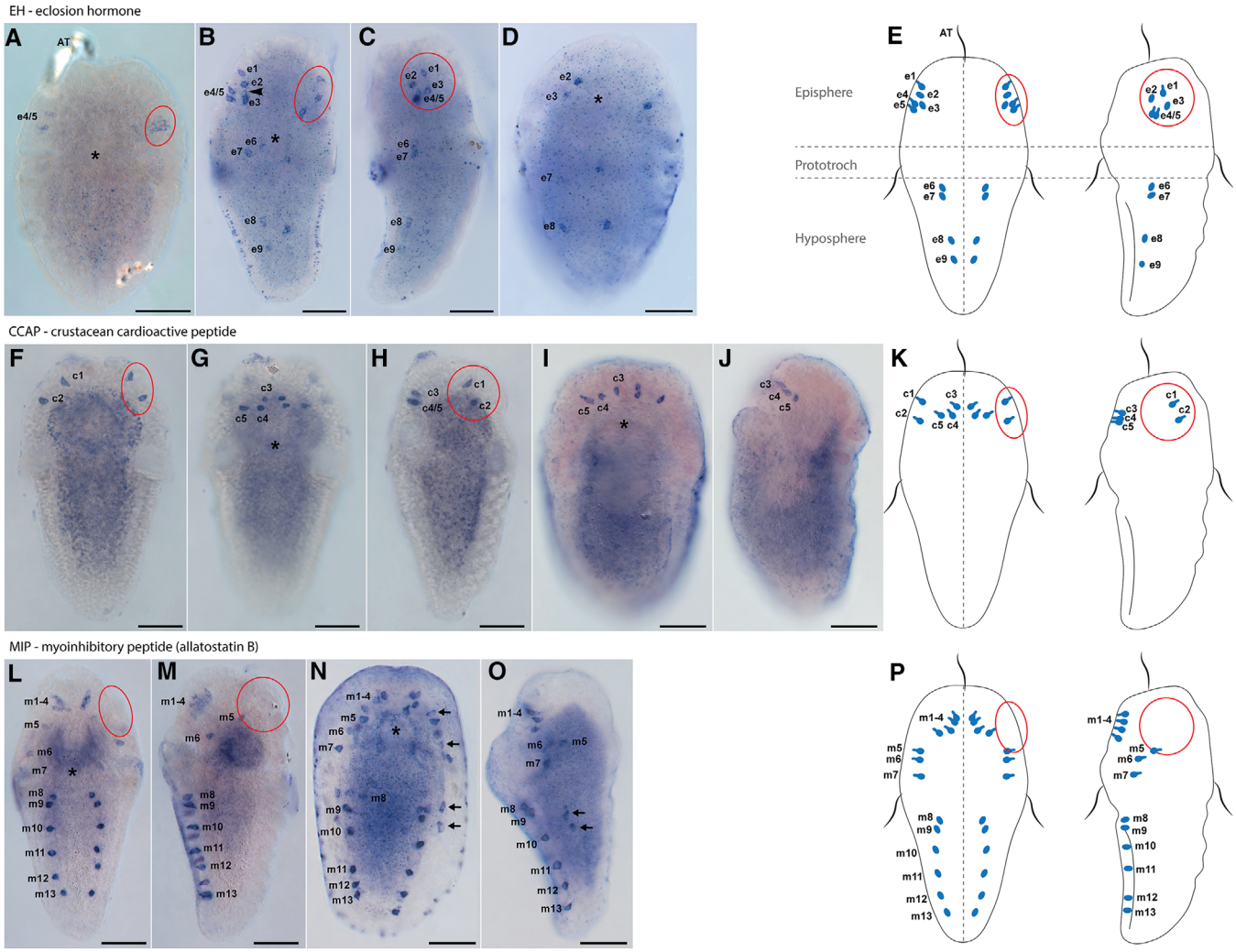

Figure 2. Developmental expression of *EH, CCAP*, and *MIP* in *Acanthochitona fascicularis*. Left: Light micrographs of larvae labeled by *in situ* hybridization. Apical faces upward. Specimens are shown in ventral view (A, B, D, G, I, L, and H), dorsal view (F), or lateral left view (C, H, J, M, O). Asterisks mark the mouth opening. Bilaterally symmetrical neuron pairs are named with the first letter of the neuropeptide they express and numbered from anterior to posterior (e.g., e1 = anterior-most pair of *EH*-expressing neuron). The location of the larval ampullary system is encircled in red. a Mid-trochophore stages (30 h) only show weak *EH* expression in the prospective ampullary system. (B-P) In competent trochophore stages (60 h, B,C,E,F-H,L,N) and early juveniles (90 h, D,I,J,N,O) transcripts of all ERNs are detected. (E,K,P) Schematics summarize ERN-expressing neurons in the late trochophore stage. Epidermal sensory neurons are mostly flask-shaped. Yolk-rich tissues inside the lecithotrophic larvae show some diffuse unspecific background staining. Scale bars: 50 μm. Abbreviations: AT, apical tuft.

juveniles, *EH* expression in basi-epidermal neurons is no longer visible (Fig. 2d, e1/4/5). Some specimens show additional cells with weak *EH* expression that are usually located in close proximity to one (or several) of the above-described neurons (i.e. Fig. 2b, arrowhead).

Crustacean cardioactive peptide (CCAP)

CCAP expression commences in late trochophore stages in five bilaterally symmetrical pairs of flask-shaped sensory neurons (Fig. 2f-h,k). Two of these *CCAP* neuron pairs are located in the lateral episphere (c1/2) in the area of the ampullary system (Friedrich et al. 2002; Haszprunar et al. 2002), while the other three are located in the ventral episphere (c3-5). In juveniles, *CCAP* expression is no longer detected laterally in c1/2 but is maintained ventrally in c3-c5 (Fig. 2i-j).

Myoinhibitory peptide (MIP)

MIP expression is first detected in late trochophore stages in 13 bilateral symmetrically arranged pairs of basi-epidermal neurons (m1-m13, Fig. 2l-m,p). While m1-4 are situated in the anterior ventral epidermis, m5-7 are located in slightly more posterior lateral positions and m8-13 are distributed along the

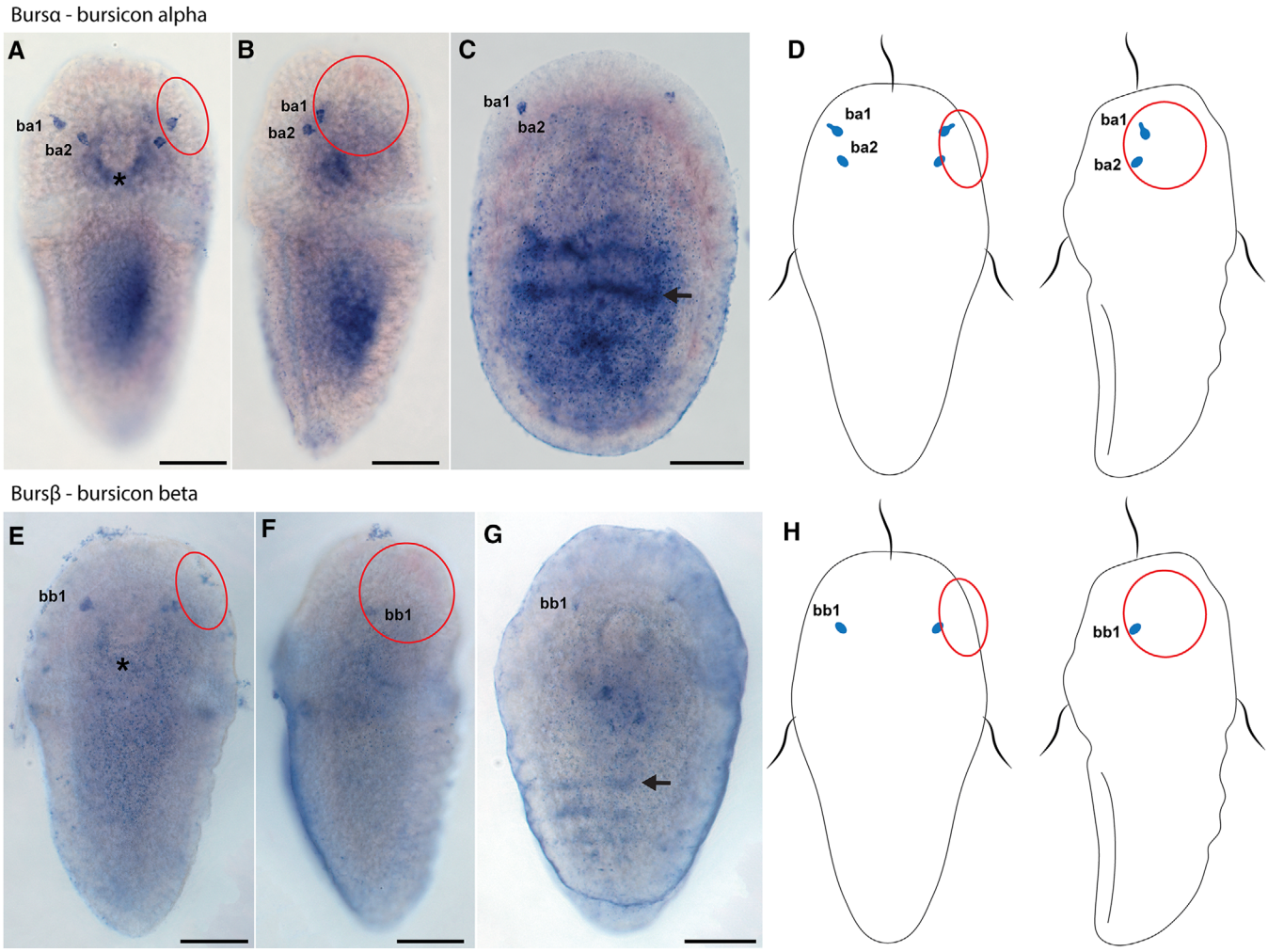

Figure 3. Developmental expression of *Bursα* and *Bursβ* in *Acanthochitona fascicularis*. Left: Light micrographs of larvae labeled by *in situ* hybridization. Apical faces upward. Specimens are shown in ventral view (A,E), dorsal view (C,G), or lateral left view (B,F). Asterisks mark the mouth opening. Bilaterally symmetrical pairs of *Bursα*- and *Bursβ*-expressing neurons are named ba and bb, respectively, and are numbered from anterior to posterior (e.g., ba1 = anterior-most pair of *Bursα*-expressing neuron). The location of the larval ampullary system is encircled in red. (A,B,E,F) *Bursα/β*-expressing neurons are detected from late trochophore stages (60 h) onward and are located lateral to the brain. (C,G) In early juveniles (90 h), *Bursα/β* expression is very faint. (D,H) Schematic summary of *Bursα/β*-expressing neurons in the late trochophore stage. Epidermal sensory neurons are mostly flask-shaped. Yolk-rich tissues inside the lecithotrophic larvae and rows of shell plate producing cells (arrows) show unspecific background staining. Scale bars: 50 μm.

ventral nerve cords. After settlement, *MIP* expression persists in the above-described cells (Fig. 2n-o). Additional neurons are present in the ventral and lateral episphere near m1-6 and in the lateral hyposphere dorsal to m8-10 (Fig. 2n-o, arrows). The latter probably correspond to lateral nerve cord neurons. In some specimens, individual *MIP* neuron pairs were missing (semi-transparent neurons, Fig. 5–7), or additional *MIP* neurons with weak and possibly transient *MIP* expression were detected (e.g., Fig. 6e-f). These variable neurons were only observed in the lateral episphere and are likely transient.

Bursicon alpha (Bursα) and bursicon beta (Bursβ)

The expression of *Bursα* and *Bursβ* starts in the late trochophore stages. *Bursα* is expressed in two pairs of bilaterally symmetrical neurons (ba1 and ba2, Fig. 3a-b,d). The ba1 neurons are located in the anterolateral epidermis and are part of the ampullary system (Fig. 3a-d), while the ba2 neurons are located in a more postero-ventral position near the brain. *Bursβ* is expressed in only one pair of neurons occupying a similar position as the ba2 neurons (bb1, Fig. 3e-h). Expression of both genes persists in juveniles (Fig. 3c,g), although only a very weak signal was obtained.

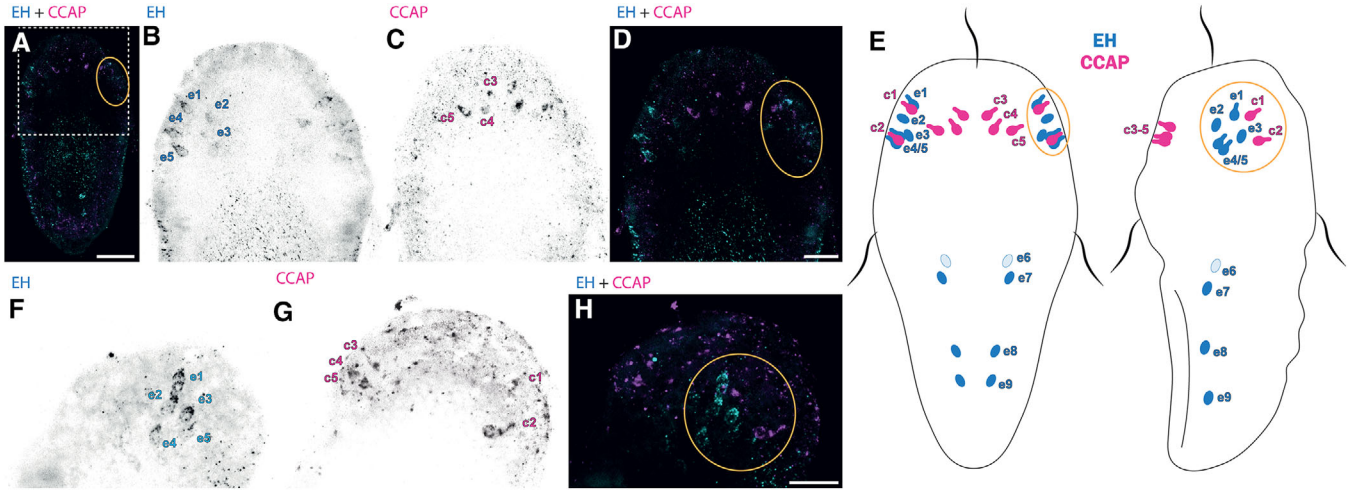

Figure 4. Co-detection of *EH* and *CCAP* expression in settlement stages of *Acanthochitona fascicularis*. Left: Confocal micrographs of settlement stages (70 h) labeled by double *in situ* hybridization against *EH* and *CCAP*. Apical faces upward. Specimens are shown in ventral view (A-D) or lateral left view (F-H). Bilaterally symmetrical pairs of neurons are named with the first letter of the neuropeptide they express and are numbered from anterior to posterior. The location of the larval ampullary system is encircled in yellow. (A) The white dashed box indicates the approximate area shown in close-ups (B-D and F-H). (B-H) No co-expression was detected, but neurons e1/4/5 and c1/2 show a similar distribution in the ampullary system of the anterolateral epidermis. (E) Schematic summary of *EH*- and *CCAP*-expressing neurons in the late trochophore stage. Semi-transparent neurons (e.g., e6) were only found in few specimens. Epidermal sensory neurons are mostly flask-shaped. Scale bars: 50 μm (A) and 25 μm (D,H).

DOUBLE LABELING REVEALS NO SPATIAL CO-EXPRESSION BUT CLOSE ASSOCIATION BETWEEN NEURONS EXPRESSING DIFFERENT ERNS

Double labeling was performed on settlement stages when ERN expression levels are particularly high (Fig. 1a). However, only a weak signal was obtained for *Bursα* and *Bursβ*, so that spatial co-expression could not be assessed for these neuropeptides. *EH, CCAP* and *MIP* are not spatially co-expressed (Fig. 4–6), but double *in situ* hybridization showed that neurons expressing these ERNs tend to cluster together. Several *EH* (e1-5, Fig. 4), *CCAP* (c1/2, Figs. 4 and 6), and *MIP* neurons (asterisks, Fig. 6) are located in close proximity to each other in the lateral episphere. These neurons correspond to the ampullary system (Fig. 4–6), an autapomorpic sensory structure of chiton larvae (Friedrich et al. 2002; Haszprunar et al. 2002). Along the ventral nerve cords, *EH* neurons (e7-9) are likewise positioned just dorsal to *MIP* neurons (m9/11/12, Fig. 5, H-K). Most notably, each *CCAP* neuron (c1-5) is in direct contact with at least one *MIP* neuron (m1-4 and asterisks, Fig. 6).

Discussion

Despite their deep conservation (de Oliveira et al. 2019; Zieger et al. 2020), surprisingly little is known about ERN expression and function outside of arthropod ecdysis (Zitnan and Adams 2012; Lee et al. 2013; Webster et al. 2013; White and Ewer 2014; Zhou et al. 2017; Oliphant et al. 2018). However, a few additional roles have been proposed for individual ERNs (An et al. 2012; Scopelliti et al. 2016; Žitňan and Daubnerová 2016; Zhang et al. 2017; Li et al. 2019; Williams 2020). Furthermore, a recent survey of temporal ERN expression profiles supports their ancestrally conserved involvement in key life cycle transitions, such as hatching and metamorphosis (Zieger et al. 2020). Consistent with this hypothesis, ERN transcript levels peak in settlement and metamorphosis stages of the polyplacophoran mollusk *A. fascicularis* (Fig. 1a).

Although major neural structures are already established in early and mid-trochophore stages (Fig. 1b-e) (Friedrich et al. 2002; Haszprunar et al. 2002; Voronezhskaya et al. 2002), our *in situ* hybridization experiments confirm that most ERN-expressing neurons form only in late trochophores, just before settlement (Figs. 2–3). Therefore, their appearance coincides with the acquisition of metamorphic competence. Some ERN-expressing neurons are lost towards the end of metamorphosis (Fig. 7), which strongly suggests that they serve a temporary purpose during this process. These data corroborate our previous findings on ERN upregulation during key life cycle events in Nephrozoa (Zieger et al. 2020).

To exert different effects, neuropeptides are released either synaptically as neurotransmitters/neuromodulators or as hormones into the circulatory system. Accordingly, arthropod ERNs are not only expressed by neurons and neurosecretory cells of the central and peripheral nervous system, but also by non-neural tissue types, including the midgut, the tracheal system, and specific

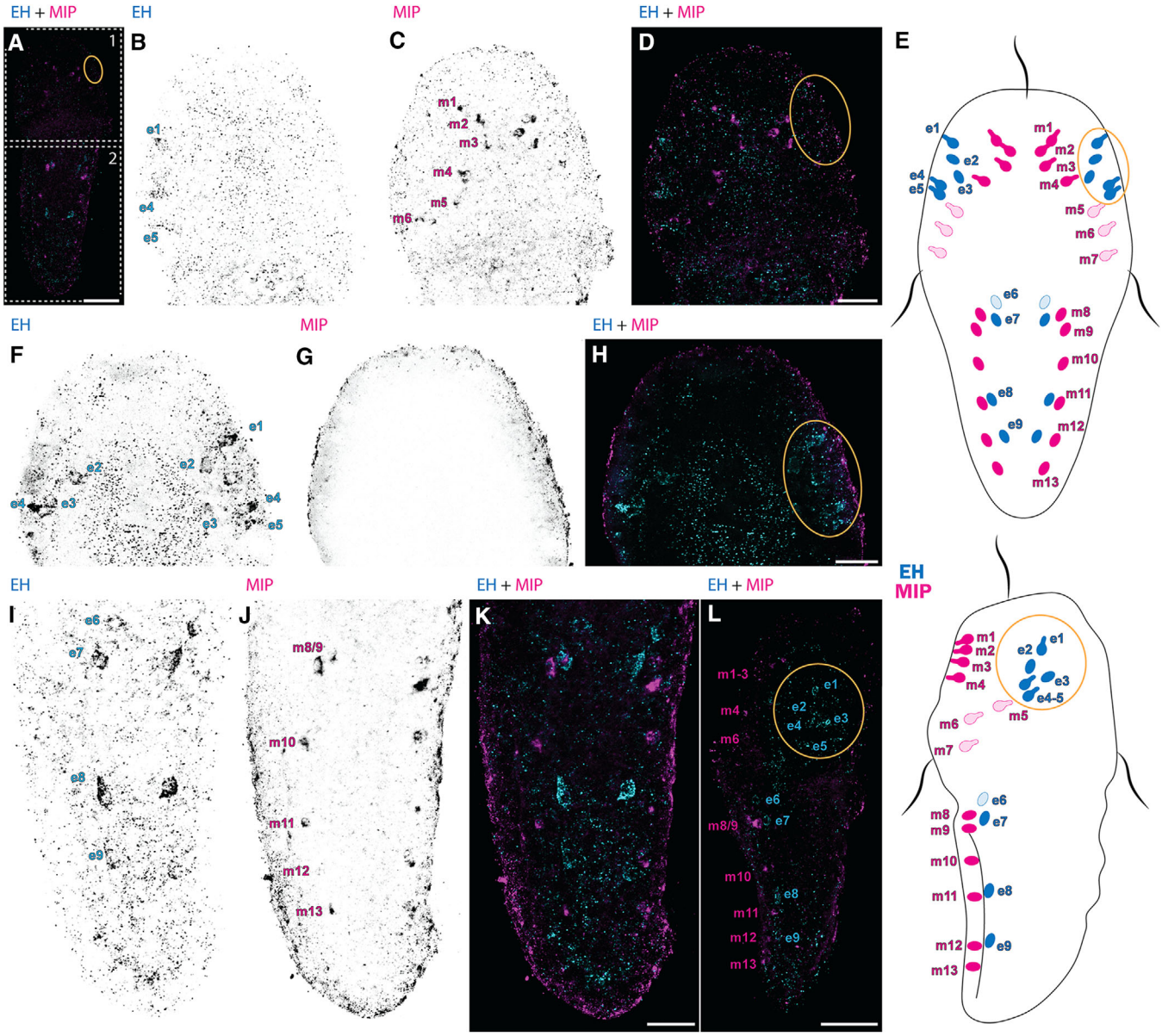

Figure 5. Co-detection of *EH* and *MIP* expression in settlement stages of *Acanthochitona fascicularis*. Left: Confocal micrographs of settlement stages (70 h) labeled by double *in situ* hybridization against *EH* and *MIP*. Apical faces upward. Specimens are shown in ventral view (A-D,I-K), dorsal view (F-H), or lateral left view (L). Bilaterally symmetrical pairs of neurons are named with the first letter of the neuropeptide they express and are numbered from anterior to posterior. The location of the larval ampullary system is encircled in yellow. (A) The white dashed boxes indicate the approximate areas shown in close-ups (B-H) (1) and (I-K) (2). b-l *EH* and *MIP* are not co-expressed, but show a similar distribution pattern along the ventral nerve cords (e6-9 and m8-13). (E) Schematic summary of *EH*- and *MIP*-expressing neurons in the late trochophore stage. Semi-transparent neurons were only found in few specimens. Epidermal sensory neurons are mostly flask-shaped. Scale bars: 50 μm (A,L) and 25 μm (D,H,K).

endocrine glands (Davis 2003; Žitňan and Daubnerová 2016; Scott et al. 2020). In contrast, *A. fascicularis* ERNs were only detected in bilateral symmetrically arranged pairs of cells, which we consider to be neurons based on their distribution and cell morphology (Fig. 7a). Here, ERNs most likely act as neurotransmitters and/or neuromodulators rather than as neurohormones. Many of these ERN-expressing neurons are flask-shaped and occupy a basi-epidermal position, which further implies sensory functions.

The larvae of *A. fascicularis* are non-feeding and most likely initiate settlement primarily based on chemical cues, as has been shown for several polyplacophoran species (Barnes and Gonor 1973; Lord 2011). Thus, the temporary *EH*- and *CCAP*-expressing neurons of the ampullary system (Fig. 7a) are prime

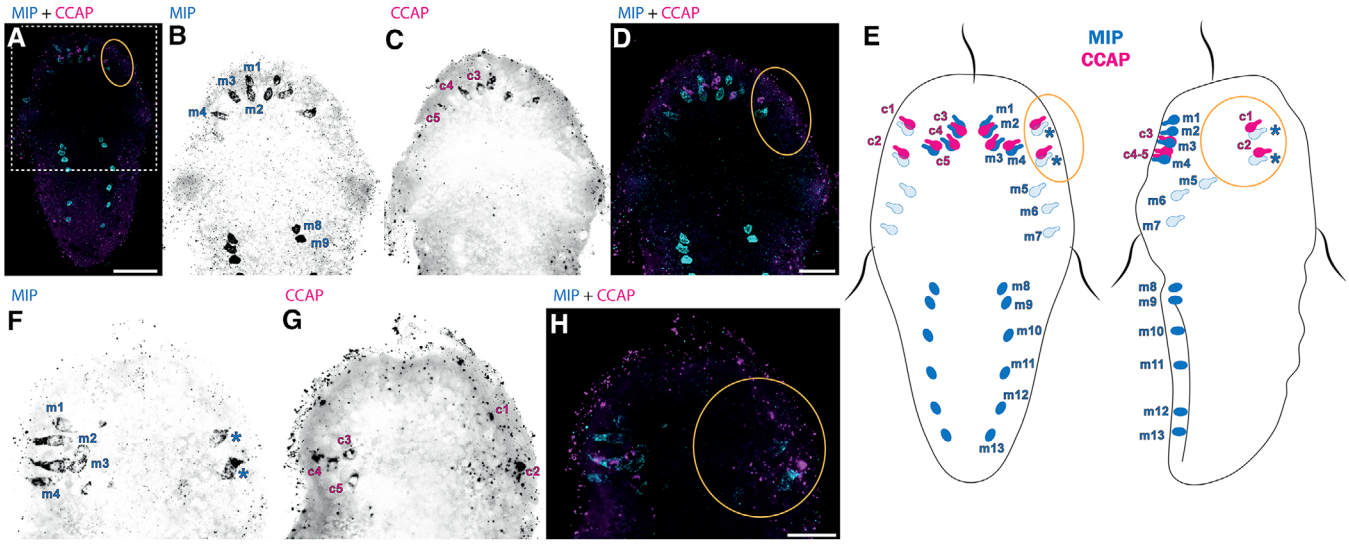

Figure 6. Co-detection of *CCAP* and *MIP* expression in settlement stages of *Acanthochitona fascicularis*. Left: Confocal micrographs of settlement stages (70 h) labeled by double *in situ* hybridization against *CCAP* and *MIP*. Apical faces upward. Specimens are shown in ventral view (A-D) or lateral left view (F-H). Bilaterally symmetrical pairs of neurons are named with the first letter of the neuropeptide they express and are numbered from anterior to posterior. The location of the larval ampullary system is encircled in yellow. (A) The white dashed box indicates the approximate area shown in close-ups (B-D and F-H). (B-F) No co-expression was observed, but each *CCAP*-expressing neuron (c1-5) is located adjacent to at least one *MIP*-expressing neuron (m1-4 and asterisks). (F) Blue asterisks indicate *MIP*-expressing neurons that were only present in few specimens. (E) Schematic summary of *CCAP*- and *MIP*-expressing neurons in the late trochophore stage. Semi-transparent neurons are only present in few specimens. Epidermal sensory neurons are mostly flask shaped. Scale bars: 50 μm (A) and 25 μm (D,H).

candidates for sensory cells that promote settlement and metamorphosis in response to suitable conditions. A similar task has been assigned to *MIP*-expressing neurons in the larval apical organ of annelids (Conzelmann et al. 2013; Hou et al. 2020). MIP-related neuropeptides of the Wamide superfamily are among the most extensively studied across metazoans and their ancestral role in metamorphic hormone signalling is well established (Schoofs and Beets 2013; Williams 2020). Yet, our findings suggest that such complex developmental transitions depend not only on MIP, but on the combined actions of several highly conserved neuropeptides, including different ERNs.

To our surprise, none of the investigated ERNs are expressed in the larval apical organ of *A. fascicularis*. The apical organ is considered responsible for controlling settlement and metamorphosis in various taxa (Kempf et al. 1997; Hadfield et al. 2000; Voronezhskaya and Khabarova 2003; Voronezhskaya et al. 2004; Rentzsch et al. 2008; Conzelmann et al. 2013; Hou et al. 2020), but its relatively early and rapid disintegration (Fig. 1, b-l, Fig. 7b) argues against a major involvement in these processes in *A. fascicularis*. A similar situation has been reported in the scaphopod *Antalis entalis*, where the larval apical organ is lost even before metamorphic competence is achieved (Wanninger and Haszprunar 2003). Moreover, a recent study on the polychaete *Hydroides elegans* showed that laser ablation of the larval apical organ does not prevent settlement and metamorphosis (Nedved et al. 2021). Accordingly, involvement in larva-to-juvenile transitions might not be as important or as widespread as is often hypothesized. Our data instead suggest that these complex developmental processes are regulated by taxon-specific sets of neurons, such as the transient ERN-expressing neurons of the polyplacophoran-specific ampullary system.

In addition to these transient neurons, other ERN-expressing cells persist in *A. fascicularis* juveniles (Fig. 7). Our RNA-seq data corroborate this observation, since juveniles maintain a relatively high expression level for most ERNs (Fig. 1). This points towards a continued requirement of ERNs, possibly for the adoption of adult-like behaviours such as feeding and crawling. Contrary to the situation in *Drosophila* (Nässel and Zandawala 2019), spatial co-expression of ERNs was not detected in *A. fascicularis*. Rather, subsets of ERN-expressing neurons are located in close proximity to one another, which suggests that they contribute to the same processes. CCAP and MIP exert myoexcitatory and myoinhibitory effects, respectively, and both have been shown to affect feeding in various animals (Žitňan and Daubnerová 2016; Williams 2020). Thus, it is likely that the abutting *CCAP*- and *MIP*-expressing neurons anterior to the mouth opening of *A. fascicularis* larvae and juveniles (Fig. 6d,h) constitute neural microcircuits that influence food-intake. Likewise, the regular arrangement of *EH*- and *MIP*-expressing neuron pairs along the ventral nerve cords corresponds to that of the seven pairs of

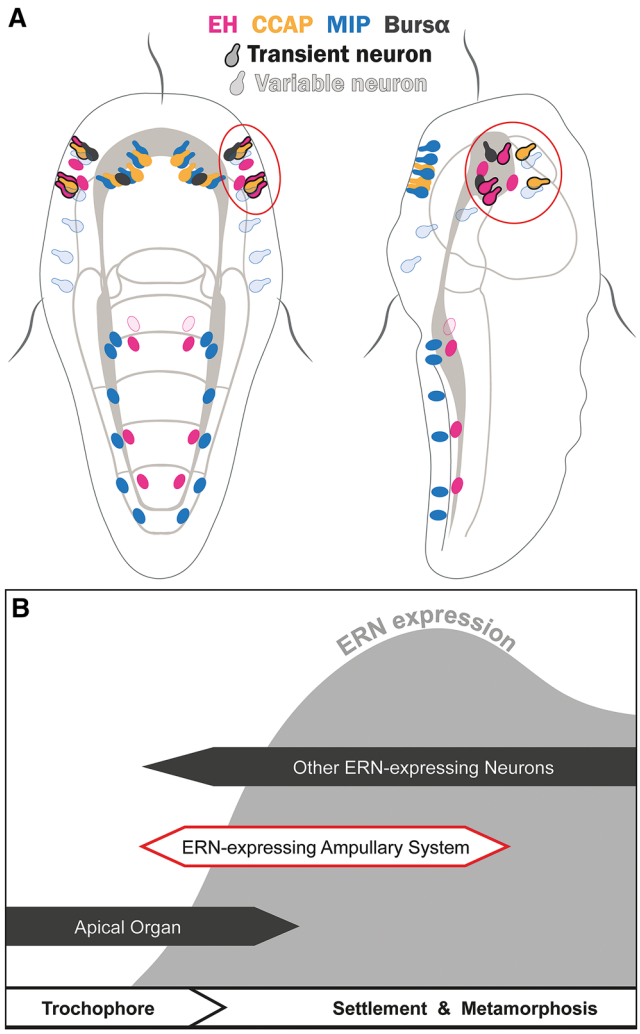

Figure 7. Ecdysis-related neuropeptide (ERNs) expression and sensory system development in *Acanthochitona fascicularis*. (A) Schematic overview of ERN-expressing neurons in the metamorphic competent trochophore larva in dorsoventral view (left) and lateral left view (right). The central nervous system and major nerve cords are indicated in light grey. Most ERN-expressing neurons (coloured shapes) are concentrated in the anterolateral ampullary system (encircled in red) and in the anterior-ventral epidermis. In addition, *EH*- and *MIP*-expressing neurons are distributed along the ventral nerve cords. Neurons outlined in black are no longer visible after metamorphosis. Semi-transparent neurons were only detected in few specimens and are probably also transient. (B) Timeline summarizing ERN expression (grey) and the presence of key sensory systems during the larva-to-juvenile transition.

dorsoventral muscle units in juvenile polyplacophorans (Wanninger and Haszprunar 2002). These dorsoventral muscles later insert on the seven juvenile shell plates, enabling defensive motor-behaviours such as curling and arching (Wanninger and Haszprunar 2002; Sigwart et al. 2019).

Importantly, a seven-fold seriality is not only typical for (larval and early juvenile) polyplacophoran muscular and skeletal elements, but is also considered ancestral for Aculifera (the monophyletic mollusk lineage that unites the polyplacophorans with the worm-like, shell-less aplacophorans) (Scherholz et al. 2013, 2015). Interspaced pairs of *MIP* neurons are also present along the ventral side of annelids (Conzelmann et al. 2013; Williams et al. 2015) and the ventral nerve cord of arthropods (Santos et al. 2007; Nässel and Zandawala 2019). Given the pre-bilaterian origin of MIP-like neuropeptides and their putative loss in deuterostomes (Williams 2020), such a pattern could be a plesiomorphic feature of protostomes that was later adapted to match different body plans and muscular arrangements. Detailed neuroanatomical comparisons between additional species will be necessary to address these deep evolutionary questions. Our findings highlight that ERNs are promising targets for this purpose due to their expression in individually identifiable neurons across protostomes.

Conclusion

Our study shows that different subsets of ERN-expressing neurons serve distinct functions during polyplacophoran development. Some are only present during settlement and metamorphosis, while others persist in juveniles and probably contribute to the onset of adult behaviours such as feeding and muscular locomotion. Consistent with data from other nephrozoan clades (Zieger et al. 2020), our findings suggest that orchestrating the larva-to-juvenile transition involves multiple ERNs in *Acanthochitona fascicularis*. Especially the transient ERN-expressing neurons of the polyplacophoran-specific and strictly larval ampullary system are likely important for this process. Absence of ERN expression in the apical organ of *A. fascicularis* as well as the relatively early and rapid loss of this structure in both polyplacophorans and scaphopods challenges the common notion that settlement and metamorphosis are chiefly regulated by the larval apical organ across protostomes. Instead, we propose that this complex task is carried out through interaction of several distinct subsets of neuropeptidergic sensory neurons, whose distributions and precise roles are likely taxon-specific, warranting further investigation in comparative studies.

AUTHOR CONTRIBUTIONS

E.Z. conceptualized the study and drafted the manuscript; C.B. and E.Z. collected the animals and carried out experiments, A.D.C., N.S.M.R. and E.Z. analysed the data; A.W. supervised the project and contributed to interpretation and discussion of the data and to finalizing the manuscript. All authors commented on and approved the final version of the manuscript.

ACKNOWLEDGMENTS

We would like to thank the Service Enseignement et Accueil Scientifique from the Station Biologique de Roscoff and the Service d'accueil de

EMBRC France for facilitating our access to important marine biological resources and research infrastructures. We would further like to thank Alexander Vogt from Vienna BioCenter Core Facilities (VBCF) for technical help with RNA-seq. The research leading to the presented results has received funding from the European Union's Horizon 2020 research and innovation program under grant agreement No 730984 to EZ. Parts of this research were supported by the Austrian Research Fund (FWF) grant P29455-B29 to AW and N.S.M.R. was supported by the Austrian Science Fund grant P3219.

DATA ARCHIVING

The *Acanthochitona fascicularis* sequence data generated and analysed during the current study are available from NCBI (BioProject ID: PRJNA706890). All other data generated or analysed during this study are included in this published article and its supporting information files. Command line details of all bioinformatic steps are provided in Data S1, Supplementary Information.

CODE AVAILABILITY

Command line details of all bioinformatic steps are provided in Data S1, Supplementary Information.

CONFLICT OF INTEREST

The authors have declared no conflict of interest.

LITERATURE CITED

An, S., S. Dong, Q. Wang, S. Li, L. I. Gilbert, D. Stanley, and Q. Song. 2012. Insect neuropeptide Bursicon homodimers induce innate immune and stress genes during molting by activating the NF-κB transcription factor Relish. PLoS ONE 7:e34510.

Barnes, J. R., and J. J. Gonor. 1973. The larval settling response of the lined chiton *Tonicella lineata*. Mar. Biol. 20:259–264.

Bray, N. L., H. Pimentel, P. Melsted, and L. Pachter. 2016. Near-optimal probabilistic RNA-seq quantification. Nat Biotechnol 34:525–527.

Bushnell, B., J. Rood, and E. Singer. 2017. BBMerge – Accurate paired shotgun read merging via overlap. PLoS ONE 12:e0185056.

Conzelmann, M., E. A. Williams, S. Tunaru, N. Randel, R. Shahidi, A. Asadulina, J. Berger, S. Offermanns, and G. Jekely. 2013. Conserved MIP receptor-ligand pair regulates *Platynereis* larval settlement. Proc Natl Acad Sci 110:8224–8229.

Davis, N. T. 2003. Localization of myoinhibitory peptide immunoreactivity in *Manduca sexta* and *Bombyx mori*, with indications that the peptide has a role in molting and ecdysis. J. Exp. Biol. 206:1449–1460.

de Oliveira, A. L., A. Calcino, and A. Wanninger. 2019. Ancient origins of arthropod moulting pathway components. eLife 8:e46113.

De Oliveira, A. L., A. Calcino, and A. Wanninger. 2019. Extensive conservation of the proneuropeptide and peptide prohormone complement in mollusks. Sci Rep 9:4846.

Ewer, J. 2005. How the ecdysozoan changed its coat. PLoS Biol 3:e349.

Friedrich, S., A. Wanninger, M. Brückner, and G. Haszprunar. 2002. Neurogenesis in the mossy chiton, *Mopalia muscosa* (Gould) (Polyplacophora): Evidence against molluscan metamerism. J. Morphol. 253:109–117.

Fritsch, M., T. Wollesen, A. L. de Oliveira, and A. Wanninger. 2015. Unexpected co-linearity of Hox gene expression in an aculiferan mollusk. BMC Evol Biol 15:151.

Fritsch, M., T. Wollesen, and A. Wanninger. 2016. Hox and ParaHox gene expression in early body plan patterning of polyplacophoran mollusks: *Lox* and *Cdx* expression in Polyplacophora. J. Exp. Zool. B Mol. Dev. Evol. 326:89–104.

Haas, B. J., A. Papanicolaou, M. Yassour, M. Grabherr, P. D. Blood, J. Bowden, M. B. Couger, D. Eccles, B. Li, M. Lieber, M. D. MacManes, M. Ott, J. Orvis, N. Pochet, F. Strozzi, N. Weeks, R. Westerman, T. William, C. N. Dewey, R. Henschel, R. D. LeDuc, N. Friedman, and A. Regev. 2013. De novo transcript sequence reconstruction from RNA-seq using the Trinity platform for reference generation and analysis. Nat Protoc 8:1494–1512.

Hadfield, M., E. Meleshkevitch, and D. Boudko. 2000. The apical sensory organ of a gastropod veliger is a receptor for settlement cues. Biol. Bull. 198:67–76.

Haszprunar, G., S. Friedrich, A. Wanninger, and B. Ruthensteiner. 2002. Fine structure and immunocytochemistry of a new chemosensory system in the chiton larva (Mollusca: Polyplacophora). J. Morphol. 251:210–218.

Hou, X., Z. Qin, M. Wei, Z. Fu, R. Liu, L. Lu, S. Bai, Y. Ma, and Z. Zhang. 2020. Identification of the neuropeptide precursor genes potentially involved in the larval settlement in the Echiuran worm *Urechis unicinctus*. BMC Genomics 21:892.

Kalyaanamoorthy, S., B. Q. Minh, T. K. F. Wong, A. von Haeseler, and L. S. Jermiin. 2017. ModelFinder: fast model selection for accurate phylogenetic estimates. Nat Methods 14:587–589.

Katoh, K., and D. M. Standley. 2013. MAFFT multiple sequence alignment software version 7: improvements in performance and usability. Mol. Biol. Evol. 30:772–780.

Kempf, S. C., L. R. Page, and A. Pires. 1997. Development of serotonin-like immunoreactivity in the embryos and larvae of nudibranch mollusks with emphasis on the structure and possible function of the apical sensory organ. J Comp Neurol 386:507–528.

Kibbe, W. A. 2007. OligoCalc: an online oligonucleotide properties calculator. Nucleic Acids Res. 35:W43–W46.

Kim, D.-H., M.-R. Han, G. Lee, S. S. Lee, Y.-J. Kim, and M. E. Adams. 2015. Rescheduling behavioral subunits of a fixed action pattern by genetic manipulation of peptidergic signaling. PLoS Genet 11:e1005513.

Lartillot, N., T. Lepage, and S. Blanquart. 2009. PhyloBayes 3: a Bayesian software package for phylogenetic reconstruction and molecular dating. Bioinformatics 25:2286–2288.

Lee, D., I. Orchard, and A. B. Lange. 2013. Evidence for a conserved CCAP-signaling pathway controlling ecdysis in a hemimetabolous insect, *Rhodnius prolixus*. Front. Neurosci. 7.

Lenaerts, C., D. Cools, R. Verdonck, L. Verbakel, J. Vanden Broeck, and E. Marchal. 2017. The ecdysis triggering hormone system is essential for successful moulting of a major hemimetabolous pest insect, *Schistocerca gregaria*. Sci Rep 7:46502.

Li, R., J. Weng, X. Wang, Q. Meng, Y. Wang, and J. Sun. 2019. Bursicon homodimers induce innate immune by activating the expression of antimicrobial peptide genes in the shrimp *Neocaridina heteropoda*. Fish Shellfish Immunol. 84:906–911.

Li, W., and A. Godzik. 2006. Cd-hit: a fast program for clustering and comparing large sets of protein or nucleotide sequences. Bioinformatics 22:1658–1659.

Lord, J. P. 2011. Larval development, metamorphosis and early growth of the gumboot chiton *Cryptochiton stelleri* (Middendorff, 1847) (Polyplacophora: Mopaliidae) on the Oregon coast. J. Molluscan Stud. 77:182–188.

Nässel, D. R., and M. Zandawala. 2019. Recent advances in neuropeptide signaling in *Drosophila*, from genes to physiology and behavior. Prog. Neurobiol. 179:101607.

Nedved, B. T., M. L. Freckelton, and M. G. Hadfield. 2021. Laser ablation of the apical sensory organ of *Hydroides elegans* (Polychaeta) does not inhibit detection of metamorphic cues. Zoology.

Nguyen, L.-T., H. A. Schmidt, A. von Haeseler, and B. Q. Minh. 2015. IQ-TREE: A Fast and Effective Stochastic Algorithm for Estimating Maximum-Likelihood Phylogenies. Mol. Biol. Evol. 32:268–274.

Oliphant, A., J. L. Alexander, M. T. Swain, S. G. Webster, and D. C. Wilcockson. 2018. Transcriptomic analysis of crustacean neuropeptide signaling during the moult cycle in the green shore crab, *Carcinus maenas*. BMC Genomics 19:711.

Pavlicek, A., T. Schwaha, and A. Wanninger. 2018. Towards a ground pattern reconstruction of bivalve nervous systems: neurogenesis in the zebra mussel *Dreissena polymorpha*. Org. Divers. Evol. 18:101–114.

Rentzsch, F., J. H. Fritzenwanker, C. B. Scholz, and U. Technau. 2008. FGF signalling controls formation of the apical sensory organ in the cnidarian *Nematostella vectensis*. Development 135:1761–1769.

Richter, S., R. Loesel, G. Purschke, A. Schmidt-Rhaesa, G. Scholtz, T. Stach, L. Vogt, A. Wanninger, G. Brenneis, C. Döring, and others. 2010. Invertebrate neurophylogeny: suggested terms and definitions for a neuroanatomical glossary. Front Zool 7:29.

Robertson, G., J. Schein, R. Chiu, R. Corbett, M. Field, S. D. Jackman, K. Mungall, S. Lee, H. M. Okada, J. Q. Qian, M. Griffith, A. Raymond, N. Thiessen, T. Cezard, Y. S. Butterfield, R. Newsome, S. K. Chan, R. She, R. Varhol, B. Kamoh, A.-L. Prabhu, A. Tam, Y. Zhao, R. A. Moore, M. Hirst, M. A. Marra, S. J. M. Jones, P. A. Hoodless, and I. Birol. 2010. De novo assembly and analysis of RNA-seq data. Nat Methods 7:909–912.

Santos, J. G., M. Vömel, R. Struck, U. Homberg, D. R. Nässel, and C. Wegener. 2007. Neuroarchitecture of peptidergic systems in the larval ventral ganglion of *Drosophila melanogaster*. PLoS ONE 2:e695.

Scherholz, M., E. Redl, T. Wollesen, C. Todt, and A. Wanninger. 2013. Aplacophoran mollusks evolved from ancestors with polyplacophoran-like features. Curr. Biol. 23:2130–2134.

Scherholz, M., E. Redl, T. Wollesen, C. Todt, and A. Wanninger. 2015. From complex to simple: myogenesis in an aplacophoran mollusk reveals key traits in aculiferan evolution. BMC Evol Biol 15:201.

Schneider, C. A., W. S. Rasband, and K. W. Eliceiri. 2012. NIH Image to ImageJ: 25 years of image analysis. Nat. Methods 9:671–675.

Schoofs, L., and I. Beets. 2013. Neuropeptides control life-phase transitions. Proc Natl Acad Sci 110:7973–7974.

Scopelliti, A., C. Bauer, J. B. Cordero, and M. Vidal. 2016. Bursicon-α subunit modulates dLGR2 activity in the adult *Drosophila melanogaster* midgut independently to Bursicon-β. Cell Cycle 15:1538–1544.

Scott, R. L., F. Diao, V. Silva, S. Park, H. Luan, J. Ewer, and B. H. White. 2020. Non-canonical eclosion hormone-expressing cells regulate *Drosophila* ecdysis. iScience 23:101108.

Shao, L., P. Chung, A. Wong, I. Siwanowicz, C. F. Kent, X. Long, and U. Heberlein. 2019. A Neural Circuit Encoding the Experience of Copulation in Female Drosophila. Neuron 102:1025-1036.e6.

Sigwart, J. D., L. H. Sumner-Rooney, E. Schwabe, M. Heß, G. P. Brennan, and M. Schrödl. 2014. A new sensory organ in "primitive" molluscs (Polyplacophora: Lepidopleurida), and its context in the nervous system of chitons. Front Zool 11:7.

Sigwart, J. D., G. J. Vermeij, and P. Hoyer. 2019. Why do chitons curl into a ball? Biol. Lett. 15:20190429.

Vinther, J. 2015. The origins of molluscs. Palaeontology 58:19–34.

Vinther, J., E. A. Sperling, D. E. G. Briggs, and K. J. Peterson. 2012. A molecular palaeobiological hypothesis for the origin of aplacophoran molluscs and their derivation from chiton-like ancestors. Proc. R. Soc. B. 279:1259–1268.

Voronezhskaya, E. E., M. Y. Khabarova, and L. P. Nezlin. 2004. Apical sensory neurones mediate developmental retardation induced by conspecific environmental stimuli in freshwater pulmonate snails. Development 131:3671–3680.

Voronezhskaya, E. E., and M. Yu Khabarova. 2003. Function of the apical sensory organ in the development of invertebrates. Dokl. Biol. Sci. 390:231–234.

Voronezhskaya, E. E., S. A. Tyurin, and L. P. Nezlin. 2002. Neuronal development in larval chiton *Ischnochiton hakodadensis* (Mollusca: Polyplacophora). J Comp Neurol 444:25–38.

Wang, D., J. Vannier, I. Schumann, X. Wang, X.-G. Yang, T. Komiya, K. Uesugi, J. Sun, and J. Han. 2019. Origin of ecdysis: fossil evidence from 535-million-year-old scalidophoran worms. Proc. R. Soc. B 286:20190791.

Wanninger, A. 2009. Shaping the things to come: ontogeny of lophotrochozoan neuromuscular systems and the tetraneuralia concept. Biol. Bull. 216:293–306.

Wanninger, A., and G. Haszprunar. 2002. Chiton myogenesis: Perspectives for the development and evolution of larval and adult muscle systems in molluscs. J. Morphol. 251:103–113.

Wanninger, A., and G. Haszprunar. 2003. The development of the serotonergic and FMRF-amidergic nervous system in *Antalis entalis* (Mollusca, Scaphopoda). Zoomorphology 122:77–85.

Wanninger, A., and T. Wollesen. 2019. The evolution of molluscs: The evolution of molluscs. Biol Rev 94:102–115.

Waterhouse, A. M., J. B. Procter, D. M. A. Martin, M. Clamp, and G. J. Barton. 2009. Jalview Version 2–a multiple sequence alignment editor and analysis workbench. Bioinformatics 25:1189–1191.

Webster, S. G., D. C. Wilcockson, Mrinalini, and J. H. Sharp. 2013. Bursicon and neuropeptide cascades during the ecdysis program of the shore crab, *Carcinus maenas*. Gen. Comp. Endocrinol. 182:54–64.

White, B. H., and J. Ewer. 2014. Neural and hormonal control of postecdysial behaviors in insects. Annu. Rev. Entomol. 59:363–381.

Williams, E. A. 2020. Function and Distribution of the Wamide Neuropeptide Superfamily in Metazoans. Front. Endocrinol. 11:344.

Williams, E. A., M. Conzelmann, and G. Jékely. 2015. Myoinhibitory peptide regulates feeding in the marine annelid *Platynereis*. Front Zool 12:1.

Wulff, J. P., N. Capriotti, and S. Ons. 2018. Orcokinins regulate the expression of neuropeptide precursor genes related to ecdysis in the hemimetabolous insect *Rhodnius prolixus*. J. Insect Physiol. 108:31–39.

Zhang, H., S. Dong, X. Chen, D. Stanley, B. Beerntsen, Q. Feng, and Q. Song. 2017. Relish2 mediates bursicon homodimer-induced prophylactic immunity in the mosquito *Aedes aegypti*. Sci Rep 7:43163.

Zhang, H.-W., G.-H. Xie, X.-H. Ren, Y.-Z. Yang, Q. Song, and H. Yu. 2020. Bursicon homodimers induce the innate immunity via Relish in *Procambarus clarkii*. Fish Shellfish Immunol. 99:555–561.

Zhou, L., S. Li, Z. Wang, F. Li, and J. Xiang. 2017. An eclosion hormone-like gene participates in the molting process of Palaemonid shrimp *Exopalaemon carinicauda*. Dev Genes Evol 227:189–199.

Zieger, E., N. S. M. Robert, A. Calcino, and A. Wanninger. 2020. Ancestral role of ecdysis-related neuropeptides in animal life cycle transitions. Curr. Biol. 31:1–7.

Zitnan, D., and M. E. Adams. 2012. Neuroendocrine regulation of ecdysis. Pp. 253–309 *in* Insect Endocrinology. Elsevier.

Žitňan, D., and I. Daubnerová. 2016. Crustacean Cardioactive Peptide. Pp. 442-e69-2 *in* Handbook of Hormones. Elsevier.

Žitňan, D., Y.-J. Kim, I. Žitňanová, L. Roller, and M. E. Adams. 2007. Complex steroid–peptide–receptor cascade controls insect ecdysis. General and Comparative Endocrinology 153:88–96.

Associate Editor: J. D. Gaitan
Handling Editor: T. Chapman

Supporting Information

Additional supporting information may be found online in the Supporting Information section at the end of the article.

Supplementary information
Supplementary information
Supplementary information